

1 **Application of the LM-BP neural network approach for**
2 **landslide risk assessments**

3 Junnan Xiong^{1,3,*}, Ming Sun², Hao Zhang¹, Weiming Cheng³, Yinghui Yang¹,
4 Mingyuan Sun¹, Yifan Cao¹ and Jiyan Wang¹

5 ¹School of Civil Engineering and Architecture, Southwest Petroleum University, Chengdu, 610500,
6 P.R. China

7 ²The First Surveying and Mapping Engineering Institute of Sichuan Province, Chengdu, 610100, P.R.
8 China

9 ³State Key Laboratory of Resources and Environmental Information System, Institute of Geographic
10 Science and Natural Resources Research, Chinese Academy of Sciences, Beijing 100101, P.R. China

11 *Correspondence to:* Junnan Xiong (neu_xjn@163.com)

12 **Running Title:** Landslide risk zonation for areas containing Products oil transport
13 **pipelines**

14

15 **Abstract.** Landslide disaster is one of the main risks involved with the operation of long-distance oil
16 and gas pipelines. Because previously established disaster risk models are too subjective, this paper
17 presents a quantitative model for regional risk assessment through an analysis of the laws of historical
18 landslide disasters along oil and gas pipelines. Using the Guangyuan section of the
19 Lanzhou-Chengdu-Chongqing (LCC) Long-Distance Products Oil Pipeline (82km) in China as a case
20 study, we successively carried out two independent assessments: a susceptibility assessment and a
21 vulnerability assessment. We used an entropy weight method to establish a system for the vulnerability
22 assessment, whereas a Levenberg Marquardt- Back Propagation (LM-BP) neural network model was
23 used to conduct the susceptibility assessment. The risk assessment was carried out on the basis of two
24 assessments. The first, the system of the vulnerability assessment, considered the pipeline position and
25 the angle between the pipe and the landslide (pipeline laying environmental factors). We also used an
26 interpolation theory to generate the standard sample matrix of the LM-BP neural network. Accordingly,
27 a landslide susceptibility risk zoning map was obtained based on susceptibility and vulnerability
28 assessment. The results showed that about 70% of the slopes were in high-susceptibility areas with a
29 comparatively high landslide possibility and that the southern section of the oil pipeline in the study
30 area was in danger. These results can be used as a guide for preventing and reducing regional hazards,
31 establishing safe routes for both existing and new pipelines and safely operating pipelines in the
32 Guangyuan section and other segments of the LCC oil pipeline.

33 **Keywords:** pipeline, landslide, risk, vulnerability, susceptibility, neural network

34

35 **1. Introduction**

36 By the year 2020, the total mileage of long-distance oil and gas pipelines is expected to exceed 160,000
37 km in China. This represents a major upsurge in the **length** of multinational long-distance oil and gas
38 pipelines (Huo, Wang, Cao, Wang, & Bureau, 2016). The rapid development of pipelines is associated
39 with significant geological hazards, especially landslides, which increasingly threaten the safe
40 operation of pipelines (P. Wang et al., 2012; Yun & Kang, 2014; Zheng, Zhang, Liu, & Wu, 2012).
41 Landslide disasters cause great harm to infrastructure and human life. Moreover, the wide impact area
42 of landslides restricts the economic development of landslide-prone areas (Ding, Heiser, Hübl, & Fuchs,
43 2016; Hong, Pradhan, Xu, & Bui, 2015). A devastating landslide can lead to casualties, property losses,
44 environmental damage and long-term service disruptions caused by massive oil and gas leakages (G. Li,
45 Zhang, Li, Ke, & Wu, 2016; Zheng et al., 2012). Generally, pipeline failure or destruction caused by
46 landslides is much more deleterious than the landslides themselves, which makes it important to
47 research the risk assessment of geological landslide hazards in pipeline areas (Inaudi & Glisic, 2006;
48 Mansour, Morgenstern, & Martin, 2011).

49 Natural disaster risk comprises a combination of natural and social attributes (Atta-Ur-Rahman &
50 Shaw, 2015). The United Nations Department of Humanitarian Affairs expresses natural disaster risk as
51 a product of susceptibility and vulnerability (Rafiq & Blaschke, 2012; Sari, Innaqa, & Safrilah, 2017).
52 In recent years, progress in geographic information systems (GIS) and remote sensing (RS)

53 technologies have greatly enhanced our ability to evaluate the potential risks that landslides pose to
54 pipelines (Akgun, Kınca, & Pradhan, 2012; B. Li & Gao, 2015; Sari et al., 2017). The disaster risk
55 assessment model has been widely recognized and applied by experts and scholars all over the world.
56 Landslide risk assessment can take the form of a qualitative (T. H. Wu, Tang, & Einstein, 1996),
57 quantitative (Ho, Leroi, & Roberds, 2000) or semi-quantitative assessment (Yingchun Liu, Shi, Lu,
58 Xiao, & Wu, 2015) according to actual demand. Quantitative methods and models that have been
59 proposed for the assessment can be divided into methods of statistical analysis (Sari et al., 2017),
60 mathematical models (Akgun et al., 2012) and machine learning (He & Fu, 2009). However, most of
61 these methods are subjective, such as expert evaluations, analytical hierarchy processes, logistic
62 regressions and fuzzy integration methods, which could affect the accuracy and reasonableness of the
63 evaluation (Fall, Azzam, & Noubactep, 2006; Sarkar & Gupta, 2005). This shortcoming can be
64 overcome through the artificial neural network, especially the mature Back Propagation (BP) Neural
65 Network that is widely used in function approximation and pattern recognition (Ke & Li, 2014a; P. L.
66 Li, Tian, & Li, 2013; Su & Deng, 2003). The evaluation indicator system generally includes disaster
67 characteristics, disaster prevention and pipeline attributes (Jianfeng Li, 2010; Shuiping Li, 2008). The
68 fault tree analysis, fuzzy comprehensive evaluation and the grey theory are used to evaluate the failure
69 probability of the system through indicator weight and scoring (Shi, 2011; Ye, Jiang, Yao, Xia, & Zhao,
70 2013). In previous studies, pipeline vulnerability evaluation indicators only considered the pipeline
71 itself, and the relationship between the pipeline and environment was rarely examined (W. Feng, Zhang,
72 & Zhang, 2014; Shuiping Li, 2008; Yingchun Liu et al., 2015). In this paper, the interaction between
73 landslide hazards and the pipeline itself was considered, which improved the quantitative degree of the
74 evaluation.

75 Based on the theory of the LM-BP neural network, a standard sample matrix was developed using
76 the interpolation theory after an analysis of the distribution characteristics of landslides that occurred in
77 the study area was performed and a regional landslide susceptibility assessment was completed.
78 Considering the interaction between landslide disasters and the pipeline itself, the pipeline vulnerability
79 evaluation in the landslide area was realized using the entropy weight method. This paper established a
80 risk assessment model and methods for assessing landslide geological susceptibility of oil pipelines by
81 comprehensively utilizing GIS and RS technology, which together improved the quantitative degree of
82 the assessment.

83 **2. Study Area**

84 The study area was Guangyuan City in the Sichuan province, which was further restricted to the area
85 from 105°15' to 106°04'E and 32°03' to 32°45'N, straddling 19 townships in five counties from south
86 to north (Figure 1). The Lanzhou-Chengdu-Chongqing (LCC) Products Oil Pipeline is China's first
87 long-distance pipeline. It begins in Lanzhou City and runs through the Shanxi and Sichuan provinces
88 (Hao & Liu, 2008). Our study area covered sloped areas of the range with 5 km on both sides of the
89 Guangyuan section (82 km) of the oil pipeline. The pipeline within the K558-K642 mileages may be
90 affected by the slope areas. The Guangyuan section, located in northern Sichuan, is a transitional zone
91 from the basin to the mountain. It features a terrain of moderate and low mountains, crisscrossed

92 networks of ravines and a strong fluvial incision. Altitudes in this area range from 328 m to 1505 m.
93 The study area has a subtropical monsoon climate with four distinctive seasons and annual
94 precipitation measuring about 900 mm to 1,000 mm. Moreover, two large unstable faults (the Central
95 Fault of Longmen Mountain and Longmen Mountain's Piedmont Fault Zone) make the area
96 geologically unstable and prone to frequent geological hazards (Shiyuan Li et al., 2012). Guangyuan,
97 through which the pipeline passes, has a high incidence of landslides, some of which have happened
98 300 times in the Lizhou and Chaotian districts (Y. Zhang, Shi, Gan, & Liu, 2011). In this area, landslide
99 geological hazards seriously threaten the safe operation of the LCC oil pipeline.

100 **3. Data Sources**

101 Landslide susceptibility assessment, pipeline vulnerability assessment and geological hazard risk
102 assessment of the landslide pipeline were made successively. Digital elevation model (DEM) data with
103 30 m accuracy was sourced from the Geospatial Data Cloud (<http://www.gscloud.cn/>). Precipitation
104 data was downloaded from the dataset of annual surface observation values in China between the years
105 1981 to 2010, as published by the China Meteorological Administration (<http://data.cma.cn/>). This data
106 was collected from 18 meteorological observatories near and within the study area and interpolated
107 using the kriging method (at a resolution of 30 m × 30 m). Geological maps and landslide data
108 (historical landslides) in the study area were obtained from the Sichuan province's geological
109 environmental monitoring station. RS images (GF-1, multispectral 8 m, resolution 2 m) were provided
110 by the Sichuan Remote Sensing Center.

111 The location of the middle line of the pipeline was detected through the direct connection method
112 (i.e., the transmitter's output line was directly connected to the metal pipeline) using an RD8000
113 underground pipeline detector. Pipeline midline coordinates were measured using total network Real
114 Time Kinematic technology, and simultaneously, the coordinates of the pipe ancillary facilities
115 (including test piles, mileage piles and milestones) were acquired. Mileage data obtained through inner
116 pipeline detection was derived from the China Petroleum Pipeline Company.

117 **4. Methods**

118 4.1 Assessment unit

119 Division precision and the scale of the slope unit (i.e., the basic element for a regional landslide
120 susceptibility assessment) were in keeping with the results of the evaluation (Qiu, Niu, ZhaoYannan, &
121 Wu, 2015). A total of 315 slope units were divided using hydrologic analysis in ArcGIS (v. 10.4) (Fig.
122 2a). The irrational unit (**slope unit with inaccurate boundary**) was artificially identified and modified by
123 comparing GF-1 satellite remote sensing images. Boundary correction, fragment combination and
124 fissure filling were used for modification.

125 **This vulnerability study focuses on assessing the vulnerability of transport pipelines to landslides**

126 Considering both previous research and the particulars of the research object, we used a comprehensive
127 segmentation method based on GIS to divide the pipelines in our study. A total of 180 pipes were
128 divided in the study area, of which the longest was about 1.7 km, and the shortest was only about 10 m
129 (Fig. 2b).

130 4.2 Assessment indicators

131 Based on selection principles of the indicator system and the formation mechanism of landslide
132 geological hazards, as few indicators as possible were selected to reflect the degree of danger posed by
133 the landslide as accurately as possible (Avalon Cullen, Al-Suhili, & Khanbilvardi, 2016; Jaiswal,
134 Westen, & Jetten, 2010; Ray, Dimri, Lakhera, & Sati, 2007). The internal factors in these indicators
135 included topography, geological structure, stratigraphic lithology and surface coverage. Similarly, the
136 external factors included mean annual precipitation (MAP) and the coefficient of the variation of
137 annual rainfall (CVAR). The correlations between indicators were analyzed using R (v. 3.3.1), and the
138 results showed a significant correlation between MAP and CVAR ($R = 0.99$) and between NDWI and
139 NDVI ($R = 0.87$). Based on correlation and standard deviation, CVAR and NDWI were eliminated
140 from the original evaluation system for landslide susceptibility assessment in the pipeline area (Table
141 1).

142 Generally, the evaluation indicator of pipeline vulnerability as it relates to the relationship between a
143 pipeline and its surrounding environment is rarely considered. The evaluation indicators in this paper
144 were refined to include pipeline parameters and the spatial relationship between a pipeline and
145 landslide. The pipelines in the study area were based in mountainous areas and had been running for
146 many years. All of these pipelines consisted of high-pressure pipes that were made of steel tubes and
147 had a diameter of 610 mm for conveying oil. In keeping with the theory of the entropy weight method,
148 these indicators (e.g., pressure, materials, diameter and media) were not included in the final
149 evaluation system used to determine pipeline vulnerability.

150 4.3 LM-BP neural network Model

151 A neural network is a nonlinear mathematical structure which is capable of representing complex
152 nonlinear processes that relate the inputs and outputs of any system (Hsu et al., 1995). With its good
153 performance on nonlinear statistical modeling, it is very useful in exploring the hidden relationships
154 between the inputs and the outputs (Z. Wu & Wang, 2016). BP Neural network with many adjustable
155 parameters has powerful parallel processing mechanism, high flexibility and can incorporate well
156 uncertainty information. The mechanism of landslide evaluation is complex, with many uncertainties
157 and incomplete information (Jie et al., 2015). The BP neural network model can find out the intrinsic
158 rules from the vast amount of complex and fuzzy data in the changing environment and make
159 corresponding inferences. The information about landslide reflected by the data used in the process of
160 susceptibility assessment is mostly qualitative rather than quantitative. Through the analysis of these
161 fuzzy information, accurate assessment results can be obtained. Landslide susceptibility assessment is
162 essentially a study of pattern recognition (F. Feng, Wu, Niu, Xu, & Yu, 2017). BP neural network can
163 approximate arbitrary continuous function with arbitrary precision, so it is widely used in non-linear
164 modeling, pattern recognition and pattern classification (Xiong, Ran, Xiong, Li, & Ye, 2010). Because
165 the BP neural network model is widely used, there are many successful cases for reference in the
166 number of neurons in each layer, the parameters of network learning and the optimization of algorithms,
167 which can effectively improve the reliability and accuracy of the model(Ke & Li, 2014b).

168 The LM algorithm, also known as the damped least square method, has the advantage of local fast

169 convergence. Its strong global searching ability contributes to the strong extrapolation ability of the
170 trained network. LM algorithm is a combination of gradient descent method and Gauss-Newton
171 method. Its iteration process is no longer along a single negative gradient direction, which greatly
172 improves the convergence speed and generalization ability of the network (Jing Li, Feng, Wang, &
173 Zhang, 2016). The BP neural network model, optimized by the LM algorithm, was used to evaluate
174 the regional landslide susceptibility in this study. MATLAB 2014 with the *trainlm* training function
175 was used to implement the LM-BP neural network. The flow chart of LM-BP neural network algorithm
176 is shown in Figure 3.

177 Data from 106 landslide disasters was collected near the research area. Of these landslides, 23 were
178 within the region of the study area. Most of the landslides located outside the study area were less than
179 20 km away from the pipeline. Due to comparable environmental conditions, these landslides could
180 still help us identify the relationship between landslides and environment factors. In light of the
181 frequency distribution of each evaluation indicator (Fig. 4), the landslide susceptibility grade
182 corresponding to each interval of the indicators was divided, and then the susceptibility degree
183 monotonicity in each interval was decided. For this study, the landslide susceptibility grade was divided
184 into four levels: low (I), medium (II), high (III) and extremely high (IV). Based on previous research
185 experience and field investigations (Appendix 8), the monotonous intervals of different indicators of
186 susceptibility degrees were judged (Appendix 1). For instance, there were hardly any landslides, only
187 collapses that occurred in slopes above 60 degrees. Besides, the susceptibility degree in the area was
188 monotone decreasing in the slope interval of 60 to 90. Because of the very small sliding force in slopes
189 at 0 degrees to 15 degrees, landslides were rare to occur here, even under other extreme conditions. (Q.
190 Zhang, Xu, Wu, & Li, 2015). On the basis of the classification criteria of the evaluation indicators used
191 to predict landslide susceptibility degree and the functional relationship between the evaluation
192 indicators and landslide probabilities, standard samples (training samples and test samples) were built
193 using a certain mathematical method. When establishing the empty matrix, the sample size of each
194 landslide susceptibility level was set to 200, and the training sample size was 800. According to the
195 order of susceptibility from low to high (Appendix 1), the input was constructed by interpolating in
196 each interval. The interval of the susceptibility degree is [0, 1], and the output is obtained by
197 interpolating 800 values equidistantly between the interval of [0, 1] (Appendix 2). Using interpolation
198 theory to build samples avoided the excess human influence in the process of building neural network
199 model by traditional methods. The training samples and test samples were evaluated using similar
200 construction methods but with different sample sizes. Finally, the indicator data was normalized, it was
201 entered into the LM-BP neural network for simulation and 315 slope unit landslide susceptibility values
202 were output.

203 4.4 Vulnerability assessment model for pipelines

204 The vulnerability evaluation model of pipelines in the landslide area was established using the entropy
205 weight method, which overcame the shortcomings of the traditional weight method that does not
206 consider the different evaluation indicators and the excessive human influence on the process of
207 evaluation (Gao, Li, Wang, Li, & Lin, 2017; Pal, 2014). Entropy is a method of measuring the

208 uncertainty of information by using probability theory (P. Liu & Zhang, 2011). The entropy indicates
 209 the extent of difference in an **indicator, the more difference the data**, the greater the role in evaluation
 210 (Jia, Zhao, Nan, & Zhao, 2007). The extremum difference method was used to normalize each indicator
 211 value. The decision information of each index can be expressed by entropy value e_i :

$$212 \quad r_{ij} = \frac{x_{ij} - \min_j \{x_{ij}\}}{\max_j \{x_{ij}\} - \min_j \{x_{ij}\}}, \quad r_{ij} = \frac{\max_j \{x_{ij}\} - x_{ij}}{\max_j \{x_{ij}\} - \min_j \{x_{ij}\}} \quad (1)$$

$$213 \quad e_i = \frac{\sum_{j=1}^n p(x_{ij}) \ln p(x_{ij})}{\ln(n)} \quad (2)$$

$$214 \quad p(x_{ij}) = \frac{r_{ij}}{\sum_{j=1}^n r_{ij}} \quad (3)$$

$$215 \quad w_i = \frac{1 - e_i}{m - \sum_{i=1}^m e_i} \quad (4)$$

$$216 \quad H_j = \sum_{i=1}^m w_i r_{ij} \quad (5)$$

217 where n is the number of evaluation objects, and r_{ij} represents the i^{th} evaluation indicator values of j^{th}
 218 pipe sections. H_j is the evaluation value of the pipeline section's vulnerability; w_i is the weight of the
 219 evaluation indicator;

220 Pipeline defect density was obtained from the pipeline internal inspection data, which consisted of
 221 both mileage data that needed to be converted into three-dimensional coordinate data and pipeline
 222 center line coordinate data obtained through C# programming. In addition, the main slide direction of
 223 the landslide was replaced by the slope direction that was extracted by DEM. The coordinate azimuth
 224 of the pipe section was extracted using the linear vector data of each pipe section, and the angle
 225 between the pipeline and the slope was calculated using the mathematical method. The calculation
 226 process was solved in the VB language on ArcGIS using second development functions. Finally, the
 227 entropy weight of 5 indicators was calculated by programming in MATLAB 2014. The entropy weight
 228 calculation results for pipeline landslide vulnerability assessment are shown in Table 2.

229

230 **5 Results and Comparison**

231 5.1 Regional landslide susceptibility assessment

232 The LM-BP neural network was trained and the network was stopped after 182 iterations. An RMSE
 233 value of 9.93e-09 indicated that the goal of precision had been reached. Through the simulation of the
 234 network test, none of the absolute error values of test data (20 groups) were found to be greater than
 235 0.02; this result aligned with our expectation of the precision of the landslide susceptibility assessment.
 236 The landslide susceptibility grade was divided into four levels by using the equal interval method at
 237 intervals of 0.25. The safe section (low susceptibility) was located in the central part of the study area.

238 The dangerous (high susceptibility) section was located north and south (Fig. 5). In the study area, most
239 of the exposed rock was dominated by shale, which belonged to the easy-slip rock group.

240 Average altitude ranged from 450 m to 1400 m, and the relative height difference was greater than
241 80 m, with the slope between 15° and 35°. Based on an overlay analysis of historic landslides within
242 the study area, and susceptibility zonation maps, we surmised that the probability of landslides in the
243 study area was extremely high, and that 87% of the landslides occurred in the medium-, high-, and
244 extremely high-susceptibility areas. Among these landslides, three were located in low-susceptibility
245 areas, which accounted for 13% of the landslide disaster sites, five occurred in medium-susceptibility
246 areas (accounting for 21.7% of disaster sites), seven occurred in high-susceptibility areas (accounting
247 for 30.4% of sites) and eight occurred in extremely high-susceptibility areas (accounting for 34.8% of
248 sites). The evaluation results were found to accurately reflect the trends and rules of distribution of
249 landslides in the study area. The number and area of slopes in high-susceptibility and extremely
250 high-susceptibility areas accounted for about 70% of the total (Table 3). The probability of landslide
251 occurrence in the study area was generally high, which was consistent with the fact that the region was
252 landslide-prone.

253 5.2 Vulnerability assessment for oil pipeline in landslide area

254 The equal interval of 0.25 was used to divide the pipeline vulnerability level into four grades to obtain
255 the pipeline vulnerability zonation of the study area (Fig. 6). The pipeline in the northern part of the
256 study area was given a low vulnerability grade, while the situation in the south of the region is more
257 serious. The number, length and percentage of pipeline segments with different grade vulnerabilities
258 are shown in Table 4. The number and length of pipeline segments in highly vulnerable areas (III) and
259 extremely vulnerable areas (IV) accounted for about 12% of the total.

260 5.3 Risk assessment for oil pipeline in landslide area

261 According to natural disaster risk expressions released by the UN, the definition of risk may be
262 expressed as the product of landslide susceptibility in a pipeline area and pipeline vulnerabilities in the
263 landslide area. Scientific analysis and expression of disaster risk assessment results can simplify
264 complex risk assessment and accelerate findings (Ding & Tian, 2013). There is no unified criterion for
265 disaster evaluation zoning, and the equal interval method is one of the methods to express the results
266 more intuitively (H. Hu, Dong, & Pan, 2011; Jin & Meng, 2011; Y. Wang, Hao, Zhao, & Fang, 2011).
267 The susceptibility and vulnerability degrees were distinguished using the equal interval method, and
268 four risk grades were then automatically generated. Where the comprehensive risk assessment value
269 was within 0 to 0.0625, the corresponding risk grade was Grade I; the corresponding risk grades with
270 the values of 0.0625 to 0.25, 0.25 to 0.5625 and 0.5625 to 1.0 were Grade II, III and IV, respectively.
271 The risk grade of each section of the pipeline within the research area is shown in Fig. 7.

272 The number of sections with a high-risk grade was 33, which accounted for 18.33% of all pipeline
273 sections and represented 16.57% of the total pipeline length of 13.461 km). There were 4 sections with
274 extremely high-risk grade, which accounted for 2.22% of all sections and represented 3.31% of the
275 total pipeline length of 2.538 km. The section number and length of pipelines lying in high-risk (III)
276 and extremely high-risk (IV) areas accounted for 20% of the total pipeline length, and the risk grade of

277 pipelines inside Qingchuan and Jian'ge County was relatively high.

278 5.4 Analysis of risk assessment results

279 Large or huge landslides were common in areas that we categorized as extremely high risk, which we
280 defined as those that were geologically evolving or had experienced obvious deformations within the
281 last 2 years with still visible cracks. These pipelines were subject to dangers at any time, as the
282 pipelines within the areas prone to landslides were found to contain many defects or extensive damage.
283 These areas also posed considerable threats; for example, pipeline ruptures or breaks could lead to
284 leakages or serious deformations that cause transportation failure. Because these are unacceptable
285 events, risk prevention and control measures must be taken in a short time. Pipelines with extremely
286 high risk were mainly distributed in the following areas: (1) Xiasi Village in Xiasi County (Pile No.
287 K628-K630); (2) Shiweng Village-Maliu Village of Xiasi County (Pile No. K635-K637). This section
288 lay in the south of the research area, with an altitude of 500 m to 750 m. Here, the slope conditions
289 affected the distribution of groundwater pore pressure and the physical and mechanical characteristics
290 of the rock and soil in three areas: vegetation cover, evaporation and slope erosion. Ultimately, these
291 three factors affected slope stability (Luo & Tan, 2011). Vertical and horizontal ravines have also
292 been seen in this section, with a relative height difference greater than 100 m and slope between
293 15° to 35°. Slope degrees with obvious changes had a great influence on slope stability (Chang & Kim,
294 2004; W. Hu, Xu, Wang, Asch, & Hicher, 2015). The exposed rocks in this area were mainly shale
295 and belonged to the sliding-prone rock group. Rock type and interlayer structure were found to be
296 important internal indicators that a landslide could occur (Guzzetti, Cardinali, & Reichenbach, 1996;
297 Xiang et al., 2010; Xin, Chong, & Dai, 2009). The distance between the fault and the pipeline in the
298 section was about 2 km with a NDVI of about 0.75 and MAP of about 970 mm. Faulted zones and
299 nearby rock and earth masses that were destroyed in a geologic event reduced the integrity of a
300 slope, and the faults and important groundwater channels could also cause deformation and
301 damage of a slope (Yinghui Liu, 2009). The pipelines in these areas exhibited many defects. Most
302 pipelines passed through the slope in an inclined or horizontal way, an attribute that typically increased
303 the risk of a landslide occurring.

304 In high-risk areas, small or moderate landslides commonly occurred in areas that we categorized as
305 high risk. They were in deformation, or had obvious deformation recently (within 2 years), such as
306 obvious cracks, subsidence or tympanites on the landslide and even shear. The pipelines in these areas
307 had defects and were buried at a shallow depth. If a landslide occurred in this pipeline area, it could
308 cause pipe suspension, floating and damage. It could also contribute to a small to moderate leakage of
309 the medium. However, damaged pipes can be welded or repaired. Monitoring is critical in high-risk
310 areas. In our study, the pipeline high-risk area was defined by the following areas: (1) Xiasi Town Xiasi
311 Village-Shiweng Village (pipe No. K622-K633). (2) Xiasi Town Maliu Village Jinzishan Xiangdasang
312 Village (pipe No. K635-K642). This area was located in the south of the pipe, which was buried in the
313 study area. The altitude of the study area was between 450 m and 800 m, the relative elevation
314 difference was over 100m and the slope was between 15° and 40°. Most of the outcrops in this area
315 were quartz sandstone, which belonged to the easy-sliding rock group. The pipes in this area were

316 about 2.5 km away from faults. The NDVI was about 0.6 to 0.8, and MAP was about 970 nm. Pipes
317 showed many defects, most of them either crossing the slope or lying in the center of slope. All of the
318 above factors provided sufficient conditions for the formation of landslide.

319 In the medium-risk areas, only small landslides were found to occur, and we observed no sign of
320 deformation. But through the analysis of geological structure, topography and landform, we found the
321 area to demonstrate a tendency for developing landslides. The pipes in this risk area exhibited almost
322 no faults and were buried deep beneath the ground. However, under bad conditions, the landslides in
323 these areas could also affect the pipes' safety, causing the pipes to become exposed or deformed. These
324 areas need simple monitoring. For our study, medium-risk areas were defined as follows: (1) Sanlong
325 village of Dongxihe township-Panlong town Dongsheng village (pipe No. K559-K593). (2) Panlong
326 town Qinlao village-Wu'ai village (pipe No. K595-K597). (3) Baolun town Laolin'gou village-Xiasi
327 town Youyu village (pipe No. K599-K630).

328 In the low-risk areas, landslides didn't occur under ordinary conditions, but they could occur if a
329 strong earthquake hit or if the area experienced continuous or heavy rain. The pipes in low-risk areas
330 showed no defects and were buried very deep. They were also located far away from areas affected by
331 landslides. Therefore, landslides in these areas caused no obvious damage to the pipes, and few
332 threatened the safety of pipes. However, regular inspection is necessary to ensure that the pipes
333 continue to operate safely. The pipe low-risk area were defined as follows: (1) Panlong town
334 Dongsheng village-Qinlao village (pipe No. K591-K597). (2) Baolun town Xiaojia village-Baolun
335 town Laolin'gou village (pipe No. K599-K608).

336 Through comprehensive analysis of each risk level area, we compiled a list of pipeline landslide
337 risks (Table 6). This list describes each landslide risk level in four respects: pipeline risk, landslide
338 susceptibility, pipeline vulnerability and risk control measures.

339 The main purpose of this study was to provide managers **and planners a comprehensive** assessment
340 **of landslide risk in areas containing pipelines**. The results offer information on the possibility of failure
341 of slopes. The landslide susceptibility maps could help planners reorganize and plan future pipeline
342 construction. Pipeline vulnerability maps could assist engineers for pipeline maintenance operation.
343 Based on this final risk map, managers and engineers can then make decisions and formulate
344 prescriptions that will have highly predictable results for safely transporting medium, settlement
345 relocation, and significantly reducing risk of any adverse effects.

346 Future research could explore detailed comparison **of different methods and recommend one or more**
347 **optimal approaches. Moreover, This study shows that landslide risk assessments can be performed with**
348 **minimal amount of relatively easy to obtain datasets. We advocate to establish a database with**
349 **assessment parameters similar as described by this study to construct dynamic landslide risk**
350 **assessment models.**

351

352 **6 Conclusion**

353 The faults inherent to traditional landslide risk assessment include excessive human influence, failure
354 of pipeline vulnerability assessments to consider the interaction between landslide disaster and pipeline

355 ontology and the low quantification degree of risk assessment results.

356 Taking the Guangyuan section (82 km) of the LCC oil and gas pipeline as an example, we used GIS
357 and RS technology to establish a regional landslide susceptibility assessment model based on the
358 LM-BP neural network. We determined that there were 112 and 108 slopes in high-susceptibility and
359 extremely high-susceptibility areas that accounted for 33.18% and 40.46% of the total area of the study
360 area, respectively. Then, we established the model of pipeline vulnerability evaluation based on the
361 entropy weight method by combining the pipeline body and the environmental information. The
362 number and length of pipe segments in the highly vulnerable (III) and extremely vulnerable area (IV)
363 accounted for about 12% of the total. Finally, based on the susceptibility assessment and the
364 vulnerability assessment, we completed the risk assessment and risk division of the oil pipeline, thus
365 forming a geological disaster risk assessment model and a method for oil pipeline and landslide risk
366 assessment. The risk assessment results demonstrated that the number and length of high-susceptibility
367 and extremely high-susceptibility pipeline segments represented 20% of the total. Similarly, the
368 pipeline risk within Qingchuan and Jian'ge Counties was relatively high. Our pipeline landslide risk
369 assessment has laid a foundation for the future study of pipeline safety management and pipeline
370 failure consequence loss assessment.

371

372 **Acknowledgments**

373 The study has been funded by the Strategic Priority Research Program of Chinese Academy of
374 Sciences (XDA20030302), IWHR(China Institute of Water Resources and Hydropower Research)
375 National Mountain Flood Disaster Investigation Project (SHZH-IWHR-57), Southwest Petroleum
376 University Of Science And Technology Innovation Team Projects (2017CXTD09) and the Study on
377 temporal and spatial differentiation of historical mountain flood disasters in Fujian province
378 (NDMBD2018003).

379

380

381 **References**

- 382 Akgun, A., Kincal, C., and Pradhan, B.: Application of remote sensing data and GIS for landslide risk
383 assessment as an environmental threat to Izmir city (west Turkey). *Environmental Monitoring &*
384 *Assessment*, 184(9), 5453-5470. [https://doi: 10.1007/s10661-011-2352-8](https://doi.org/10.1007/s10661-011-2352-8) 2012.
- 385 Atta-Ur-Rahman, and Shaw, R. (2015). *Hazard, Vulnerability and Risk: The Pakistan Context*: Springer
386 Japan.
- 387 Avalon Cullen, C., Al-Suhili, R., and Khanbilvardi, R.: Guidance Index for Shallow Landslide Hazard
388 Analysis. *Remote Sensing*, 8(10), 866. [https://doi: 10.3390/rs8100866](https://doi.org/10.3390/rs8100866), 2016.
- 389 Chang, H., and Kim, N. K.: The evaluation and the sensitivity analysis of GIS-based landslide
390 susceptibility models. *Geosciences Journal*, 8(4), 415-423. [https://doi: 10.1007/BF02910477](https://doi.org/10.1007/BF02910477), 2004.
- 391 Ding, M., Heiser, M., Hübl, J., and Fuchs, S.: Regional vulnerability assessment for debris flows in
392 China—a CWS approach. *Landslides*, 13(3), 537-550. [https://doi: 10.1007/s10346-015-0578-1](https://doi.org/10.1007/s10346-015-0578-1) 2016.
- 393 Ding, M., and Tian, S. (2013). *Landslide and Debris Flow Risk Assessment and Its Application* Beijing:
394 Science Press.
- 395 Fall, M., Azzam, R., and Noubactep, C.: A multi-method approach to study the stability of natural
396 slopes and landslide susceptibility mapping. *Engineering Geology*, 82(4), 241-263. 2006.
- 397 Feng, F., Wu, X., Niu, R., Xu, S., and Yu, X.: Landslide susceptibility assessment based on PSO-BP
398 neural network. *Science of Surveying*
399 *Mapping*, 42(10), 170-175. [https://doi: 10.16251/j.cnki.1009-2307.2017.10.027](https://doi.org/10.16251/j.cnki.1009-2307.2017.10.027), 2017.
- 400 Feng, W., Zhang, T., and Zhang, Y.: Evaluating the stability of landslides in xianshizhai village and the
401 pipeline vulnerability with their action. *Journal of Geological Hazards & Environment Preservation*.
402 2014.
- 403 Gao, C. L., Li, S. C., Wang, J., Li, L. P., and Lin, P.: The Risk Assessment of Tunnels Based on Grey
404 Correlation and Entropy Weight Method. *Geotechnical & Geological Engineering*(4), 1-11. [https://doi:](https://doi.org/10.1007/s10706-017-0415-5)
405 [10.1007/s10706-017-0415-5](https://doi.org/10.1007/s10706-017-0415-5) 2017.
- 406 Guzzetti, F., Cardinali, M., and Reichenbach, P.: The Influence of Structural Setting and Lithology on
407 Landslide Type and Pattern. *Environmental & Engineering Geoscience*, 2(4), 531-555. 1996.
- 408 Hao, J., and Liu, J.: Zonation of Danger Degree of Geological Hazards over
409 Lanzhou-Chengdu-Chongqing Products Pipeline. *Oil & Gas Storage & Transportation*. 2008.
- 410 He, Y., and Fu, W.: Application of fuzzy support vector machine to landslide risk assessment. *Journal*
411 *of Natural Disasters*, 18(5), 107-112. 2009.
- 412 Ho, K., Leroi, E., and Roberds, B.: *Quantitative Risk Assessment : Application, Myths and Future*
413 *Direction*. 2000.
- 414 Hong, H., Pradhan, B., Xu, C., and Bui, D. T.: Spatial prediction of landslide hazard at the Yihuang
415 area (China) using two-class kernel logistic regression, alternating decision tree and support vector
416 machines. *Catena*, 133, 266-281. [https://doi: 10.1016/j.catena.2015.05.019](https://doi.org/10.1016/j.catena.2015.05.019) 2015.
- 417 Hsu, K. L. , Gupta, H. V. , & Sorooshian, S.: **Artificial neural network modeling of the rainfall-runoff**
418 **process. *Water Resources Research*, 31(10), 2517-2530, doi: 10.1029/95WR01955, 1995.**
- 419 Hu, H., Dong, P., and Pan, j.: The Hail Risk Zoning in Beijing Integrated with the Result of Its Loss
420 Assessment. *Journal of Applied Meteorological Science*, 22(5), 612-620. 2011.
- 421 Hu, W., Xu, Q., Wang, G. H., Asch, T. W. J. V., and Hicher, P. Y.: Sensitivity of the initiation of debris
422 flow to initial soil moisture. *Landslides*, 12(6), 1139-1145. [https://doi: 10.1007/s10346-014-0529-2](https://doi.org/10.1007/s10346-014-0529-2)
423 2015.
- 424 Huo, F., Wang, W., Cao, Y., Wang, F., and Bureau, C. P.: *China's Construction Technology of Oil and*

425 Gas Storage and Transportation and Its Future Development Direction. *Oil Forum*. 2016.

426 Inaudi, D., and Glisic, B.: Reliability and field testing of distributed strain and temperature sensors.

427 *Proceedings of SPIE - The International Society for Optical Engineering*, 6167(14), 2586–2597.

428 [https://doi: 10.1117/12.661088](https://doi.org/10.1117/12.661088) 2006.

429 Jaiswal, P., Westen, C. J. V., and Jetten, V.: Quantitative landslide hazard assessment along a

430 transportation corridor in southern India. *Engineering Geology*, 116(3), 236-250. [https://doi:](https://doi.org/10.1016/j.enggeo.2010.09.005)

431 [10.1016/j.enggeo.2010.09.005](https://doi.org/10.1016/j.enggeo.2010.09.005), 2010.

432 Jia, Y., Zhao, J., Nan, Z., and Zhao, C.: The Application of Entropy-right Method to the Study of

433 Ecological Security Evaluation of Grassland—A Case Study at the Ecological Security Evaluation of

434 Grassland to Pastoral Area of Gansu.

435 *Journal of Arid Land Resources*

436 *Environmental & Engineering Geoscience*. [https://doi: 10.1016/S1872-5791\(08\)60002-0](https://doi.org/10.1016/S1872-5791(08)60002-0) 2007.

437 Jie, D., Yamagishi, Hiromitsu, Reza, P. H., Yunus, A. P., Xuan, S., Xu, Y., and Zhu, Z.: An integrated

438 artificial neural network model for the landslide susceptibility assessment of Osado Island, Japan.

439 *Natural Hazards*, 78(3), 1749-1776. 2015.

440 Jin, Y., and Meng, J. J.: Assessment and forecast of ecological vulnerability:A review. *Chinese Journal*

441 *of Ecology*, 30(11), 2646-2652. 2011.

442 Ke, F., and Li, Y.: The forecasting method of landslides based on improved BP neural network.

443 *Geotechnical Investigation & Surveying*. 2014a.

444 Ke, F., and Li, Y.: The forecasting method of landslides based on improved BP neural network.

445 *Geotechnical Investigation*

446 *Surveying*, 42(8), 55-60. 2014b.

447 Li, B., and Gao, Y. (2015). Application of the improved fuzzy analytic hierarchy process for landslide

448 hazard assessment based on RS and GIS. Paper presented at the International Conference on Intelligent

449 Earth Observing and Applications.

450 Li, G., Zhang, P., Li, Z., Ke, Z., and Wu, G.: Safety length simulation of natural gas pipeline subjected

451 to transverse landslide. 2016.

452 Li, J. (2010). Wenchuan Earthquake and Secondary Geological Hazard Assessment Based on RS/GIS

453 Technology. (Master), China University of Geosciences, Beijing, China.

454 Li, J., Feng, J., Wang, W., and Zhang, F.: Spatial and Temporal Changes in Solar Radiation of

455 Northwest China Based LM-BP Neural Network. *Scientia Geographica Sinica*, 36(5), 780-786.

456 [https://doi: 10.13249/j.cnki.sgs.2016.05.017](https://doi.org/10.13249/j.cnki.sgs.2016.05.017), 2016.

457 Li, P. L., Tian, W. P., and Li, J. C.: Analysis of landslide stability based on BP neural network. *Journal*

458 *of Guangxi University*. 2013.

459 Li, S. (2008). The Risk Assessment Study on the Environmental Geological Hazards along the

460 West-East Nature Gas Pipeline. (Mater), SouthWest JiaoTong University, Chengdu, China.

461 Li, S., Jian, j., Wu, Z., Li, S., Li, H., Bai, K., Ke, Q., Xu, Y., and Hu, Y.: A Design of the

462 Geo-Environmental Management Database System for Guangyuan City *Journal of Geological Hazards*

463 *and Environment Preservation*, 23(3), 7. 2012.

464 Liu, P., and Zhang, X.: Research on the supplier selection of a supply chain based on entropy weight

465 and improved ELECTRE-III method. *International Journal of Production Research*, 49(3), 637-646.

466 [https://doi: 10.1080/00207540903490171](https://doi.org/10.1080/00207540903490171), 2011.

467 Liu, Y. (2009). The characteristic and evaluation of collapse and landslide disaster along du-wen

468 highway in Wenchuan earthquake region. (Master), Lanzhou University, Lanzhou.

469 Liu, Y., Shi, Y., Lu, Q., Xiao, H., and Wu, S.: Risk Assessment of Geological Disasters in Single Pipe
470 Based on Scoring Index Method: A Case Study of Soil Landslide. *Natural Gas Technology & Economy*.
471 2015.

472 Luo, Z. F., and Tan, D. J.: Landslide Hazard Evaluation in Debris Flow Catchment Area Based on GIS
473 and Information Method. *China Safety Science Journal*, 21(11), 144-150. [https://doi:
474 10.1631/jzus.B1000265](https://doi:10.1631/jzus.B1000265) 2011.

475 Mansour, M. F., Morgenstern, N. R., and Martin, C. D.: Expected damage from displacement of
476 slow-moving slides. *Landslides*, 8(1), 117-131. [https://doi: 10.1007/s10346-010-0227-7](https://doi:10.1007/s10346-010-0227-7) 2011.

477 Pal, R.: Entropy Production in Pipeline Flow of Dispersions of Water in Oil. *Entropy*, 16(8), 4648-4661.
478 [https://doi: 10.3390/e16084648](https://doi:10.3390/e16084648) 2014.

479 Qiu, D., Niu, R., ZhaoYannan, and Wu, X.: Risk Zoning of Earthquake-Induced Landslides Based on
480 Slope Units:A Case Study on Lushan Earthquake. *Journal of Jilin University*, 45(5), 1470-1478.
481 [https://doi: 10.13278/j.cnki.jjuese.201505201](https://doi:10.13278/j.cnki.jjuese.201505201) 2015.

482 Rafiq, L., and Blaschke, T.: Disaster risk and vulnerability in Pakistan at a district level. *Geomatics
483 Natural Hazards & Risk*, 3(4), 324-341. [https://doi: 10.1080/19475705.2011.626083](https://doi:10.1080/19475705.2011.626083) 2012.

484 Ray, P. K. C., Dimri, S., Lakhera, R. C., and Sati, S.: Fuzzy-based method for landslide hazard
485 assessment in active seismic zone of Himalaya. *Landslides*, 4(2), 101. [https://doi:
486 10.1007/s10346-006-0068-6](https://doi:10.1007/s10346-006-0068-6) 2007.

487 Sari, D. A. P., Innaqa, S., and Safriolah. Hazard, Vulnerability and Capacity Mapping for Landslides
488 Risk Analysis using Geographic Information System (GIS). 209(1), 012106. [https://doi:
489 10.1088/1757-899X/209/1/012106](https://doi:10.1088/1757-899X/209/1/012106) 2017.

490 Sarkar, S., and Gupta, P. K.: Techniques for Landslide Hazard Zonation – Application to
491 Srinagar-Rudraprayag Area of Gar. *Journal of the Geological Society of India*, 65(2), 217-230. 2005.

492 Shi, S.: Risk Analysis for Pipeline Construction about Third Party Damage Based on Triangular Fuzzy
493 Number and Fault Tree Theory. *Journal of Chongqing University of Science & Technology*. 2011.

494 Su, G., and Deng, F.: On the Improving Backpropagation Algorithms of the Neural Networks Based on
495 MATLAB Language:A Review. *Bulletin of Science & Technology*. 2003.

496 Wang, P., Xu, Z., Bai, M., Du, Y., Mu, S., Wang, D., and Yang, Y.: Landslide Risk Assessment Expert
497 System Along the Oil and Gas Pipeline Routes. *Advanced Materials Research*, 418-420, 1553-1559.
498 [https://doi: 10.4028/www.scientific.net/AMR.418-420.1553](https://doi:10.4028/www.scientific.net/AMR.418-420.1553) 2012.

499 Wang, Y., Hao, J., Zhao, F., and Fang, L.: A Discussion on Regional Risk Zoning of Geological Hazard
500 in the Worst-hit Area of the Wenchuan Earthquake in Shaanxi Province. *Journal of Catastrophology*,
501 26(4), 35-39. [https://doi: 10.1007/s12583-011-0163-z](https://doi:10.1007/s12583-011-0163-z), 2011.

502 Wu, T. H., Tang, W. H., and Einstein, H. H. (1996). *Landslides: investigation and mitigation*. chapter 6
503 - landslide hazard and risk assessment.

504 Wu, Z., and Wang, H.: Super-resolution Reconstruction of SAR Image based on Non-Local Means
505 Denoising Combined with BP Neural Network. 2016.

506 Xiang, L. Z., Cui, P., Zhang, J. Q., Huang, D. C., Fang, H., and Zhou, X. J.: Triggering factors
507 susceptibility of earthquake-induced collapses and landslides in Wenchuan County. *Journal of Sichuan
508 University*, 42(5), 105-112. 2010.

509 Xin, Y., Chong, X. U., and Dai, F. C.: Contribution of strata lithology and slope gradient to landslides
510 triggered by Wenchuan Ms 8 earthquake,Sichuan,China. *Geological Bulletin of China*, 28(8),
511 1156-1162. 2009.

512 Xiong, H., Ran, Y., Xiong, G., Li, S., and Ye, L.: Study on deformation prediction of landslide based on

513 genetic algorithm and improved BP neural network. *Kybernetes the International Journal of Systems*
514 *Cybernetics*, 39(8), 1245-1254. 2010.

515 Ye, C., Jiang, H., Yao, A., Xia, Q., and Zhao, X.: Study on risk controlling method of third party
516 construction damage on oil and gas pipeline. *Journal of Safety Science & Technology*, 9(8), 140-145.
517 2013.

518 Yun, L., and Kang, L.: Reliability Analysis of High Pressure Buried Pipeline under Landslide. *Applied*
519 *Mechanics & Materials*, 501-504, 1081-1086. [https://doi:](https://doi.org/10.4028/www.scientific.net/AMM.501-504.1081)
520 [10.4028/www.scientific.net/AMM.501-504.1081](https://doi.org/10.4028/www.scientific.net/AMM.501-504.1081) 2014.

521 Zhang, Q., Xu, Q., Wu, L., and Li, J.: BP neural network model for forecasting volume of landslide
522 group in Nanjiang. *Hydrogeology and Engineering Geology*, 42(1), 6. 2015.

523 Zhang, Y., Shi, J., Gan, J., and Liu, C.: Analysis of Distribution Characteristics and Influencing Factors
524 of Secondary Geohazards in Guangyuan City—Taking Chaotian District as an Example. *Journal of*
525 *Catastrophology*, 26(1), 75-79. [https://doi: 10.1007/s12182-011-0118-0](https://doi.org/10.1007/s12182-011-0118-0) 2011.

526 Zheng, J. Y., Zhang, B. J., Liu, P. F., and Wu, L. L.: Failure analysis and safety evaluation of buried
527 pipeline due to deflection of landslide process. *Engineering Failure Analysis*, 25(4), 156-168.
528 [https://doi: 10.1016/j.engfailanal.2012.05.011](https://doi.org/10.1016/j.engfailanal.2012.05.011) 2012.

529

530 **List of tables and figures**

531 **Table 1** Indicators of landslide susceptibility assessment and pipeline vulnerability assessment

532 **Table 2** Entropy weight of evaluation indicator

533 **Table 3** Number and area of slopes of four hazard grade

534 **Table 4** Number and distances of pipeline of four vulnerability grade

535 **Table 5** Number and distances of pipeline of four risk grade

536 **Table 6** Description of pipeline risk level

537

538 **Figure 1** Landslide location map of the study area

539 **Figure 2** All slope units (a) and pipeline section (b) in the study area

540 **Figure 3** Flow chart of LM-BP neural network algorithm

541 **Figure 4** The frequency distribution of each indicator in the landslide location. Maps (a), (b), (c), (d),

542 (e), (f), (g), and (h) represent the elevation, slope, aspect, height difference, TPC, NVI, MAP, and

543 distance from the fault, respectively

544 **Figure 5** Landslide hazard map of study area

545 **Figure 6** Pipeline vulnerability map of study area

546 **Figure 7** Pipeline risk map of study area

547

548
 549
 550
 551
 552
 553
 554
 555
 556

Table 1

	Factor	Indicators
Landslide hazard indicator	Landform	Elevation
		Slope
		Aspect
		Height Difference
	Land cover	Topographic profile curvature (TPC)
		NDVI
		NDWI
Geology	Lithology	
	Distance from the fault	
Precipitation	Mean annual precipitation (MAP)	
	Coefficient of variation of annual rainfall (CVAR)	
Pipeline vulnerability indicator	Pipe Body	Defect Density
		Depth
		Thickness
		Pressure
		Materials
		Diameter
	Spatial relationship between pipeline and landslide	Media
	Position	
	Angle	

557
 558
 559

560
561
562
563
564
565
566
567
568
569
570
571
572
573
574

Table 2

	Depth	Angle	Defect Density	Thickness	Position
Weight	0.010007	0.101553	0.678851	0.154322	0.055266
Entropy	0.997322	0.97282	0.818308	0.958696	0.985208

575
576

577

Table 3

Landslide susceptibility	Number of slopes	Percentage (%)	Area (km²)	Percentage (%)
Low (I)	33	10.48	32.63	8.76
Medium (II)	62	19.68	65.53	17.60
High (III)	112	35.56	123.55	33.18
Extremely high (IV)	108	34.29	150.65	40.46
Total	315	100	372.36	100

578

579

580

Table 4

Pipeline vulnerability	Number of pipelines	Percentage (%)	Area (km ²)	Percentage (%)
Low (I)	120	66.66	50.417	62.06
Medium (II)	37	20.56	20.888	25.72
High (III)	22	12.22	9.833	12.11
Extremely (IV)	1	0.56	0.087	0.11
Total	180	100	81.225	100

581

582

583

Table 5

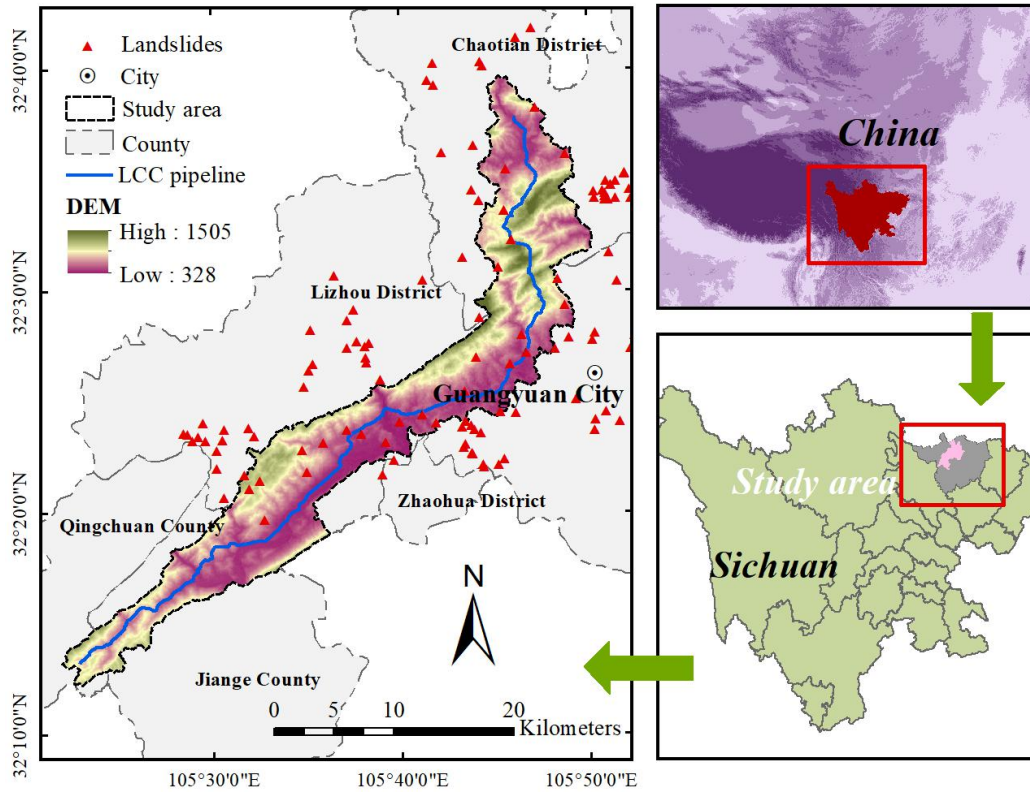
Pipeline risk	Number of pipelines	Percentage (%)	Area (km ²)	Percentage (%)
Low (I)	37	20.56	14.469	17.81
Medium (II)	106	58.89	50.757	62.49
High (III)	33	18.33	13.461	16.57
Extremely (IV)	4	2.22	2.538	3.13
Total	180	100	81.225	100

584

585

Table 6

Pipeline risk	Landslides susceptibility	Vulnerability	Risk	Control measures
Low (I)	The landslide won't happen under ordinary conditions, but it will occur when strong earthquake, long continuous rain or extremely heavy rain happened.	The pipes in low risk areas have no any defects and buried very deep. Meanwhile, they are far away from the area affected by landslide.	Landslides have no obvious damage to the pipes, and few threats to pipes' safety.	Regular Inspection
Medium (II)	Small landslide mainly occur, and no sign of deformation. But through analyzing geological structure, topography and landform, there is a tendency of landslide.	The pipes in risk areas have almost no faults and buried deep. However, under bad condition, the landslide may also affect the pipes' safety.	The landslide may make the pipes exposed or deformation.	simple monitoring
High (III)	Landslides are most in medium-model and little-model, and they are in deformation, or have obvious deformation recently, such as obvious cracks, subsidence or tympanites on the landslide and even shear.	The pipeline has defects, and buried shallow. Once landslides occurred in the pipeline area, pipes' safety will be threatened	The safety of pipeline will be threatened and may suffer from pipe suspension, floating, and damage etc. Therefore it will contribute to a small amount of medium leakage. Fortunately, the pipe can be welded or repaired.	Main monitoring
Extremely high (IV)	Large or huge landslide is common in the area with extremely high risk, which is changing or has experienced obvious deformation recently with visible cracks.	The pipelines are subject to dangers at any time as the pipelines within the area prone to landslide have been spotted with many defects or much damage.	There are great threats, for example pipeline rupture or break and may lead to considerable leakage of media or serious deformation even transportation failure.	Prevention and control measures shall be taken in a short time



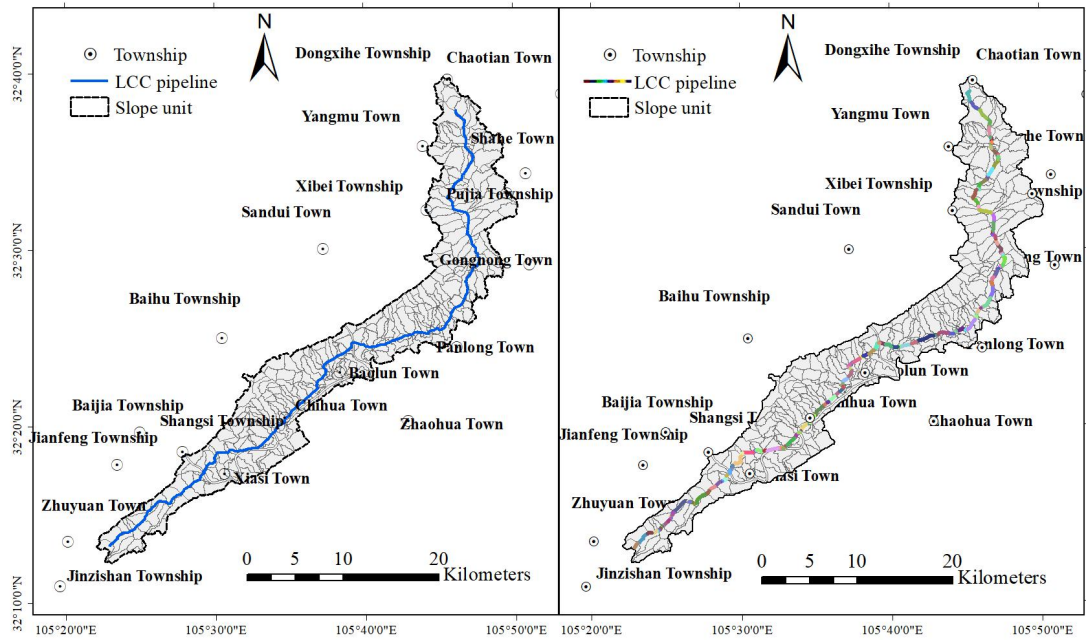
589

590

591

592

Figure 1

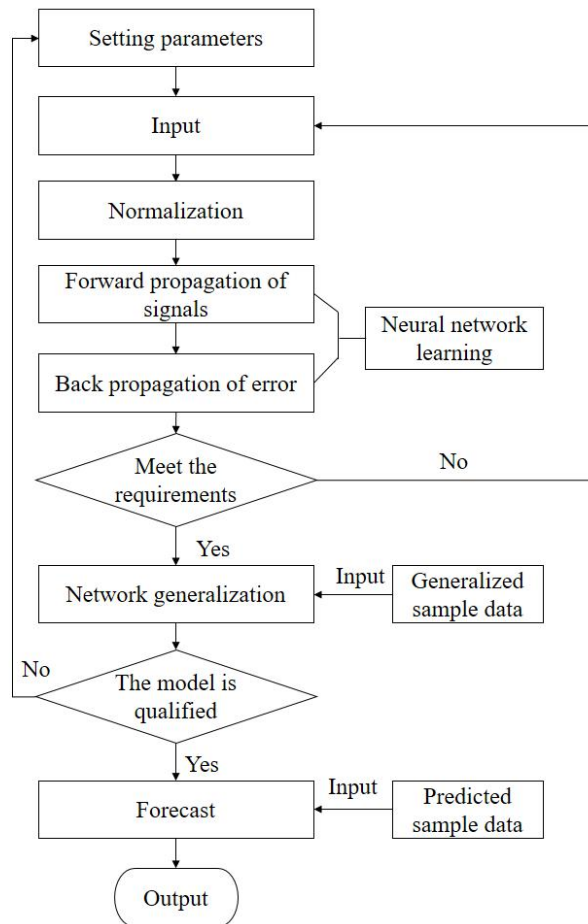


593

594

595

Figure 2



596

597

598

Figure 3

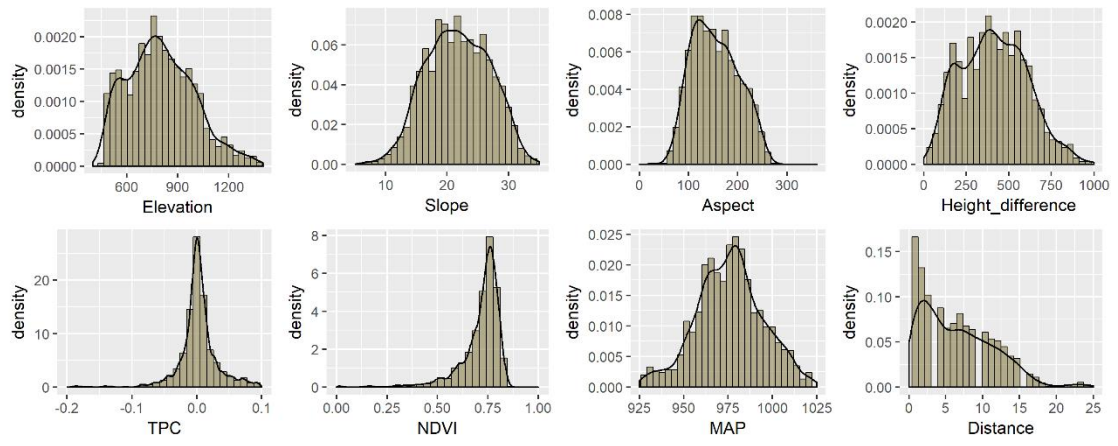


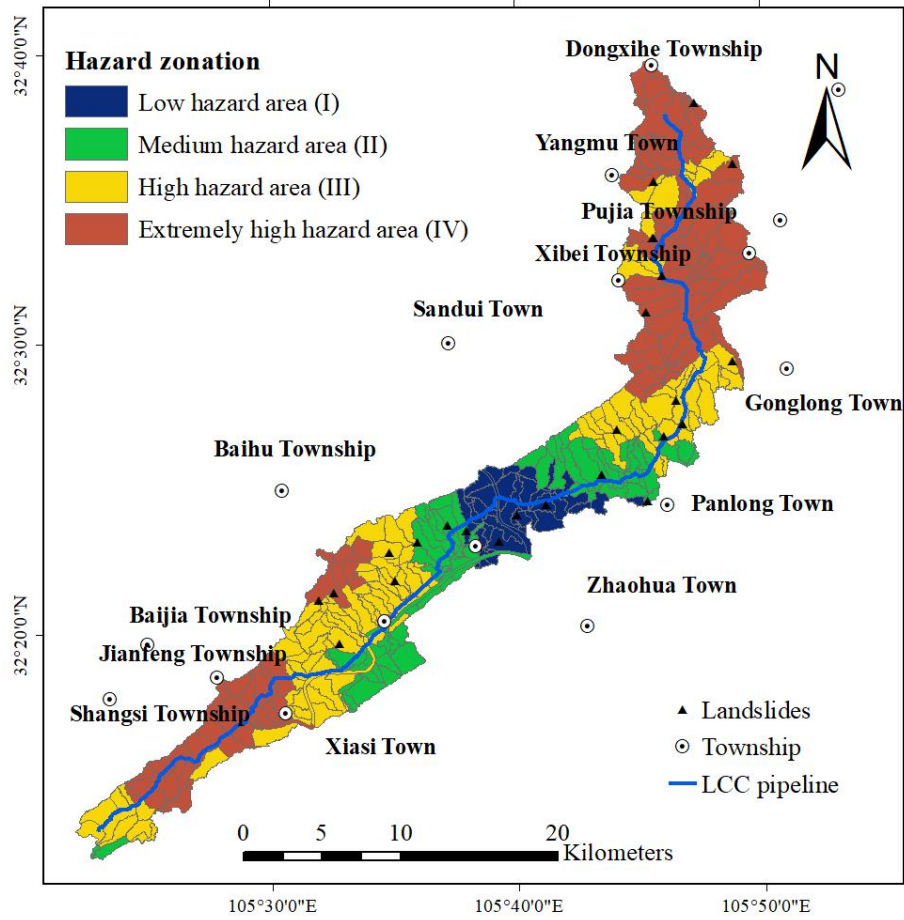
Figure 4

599

600

601

602



603

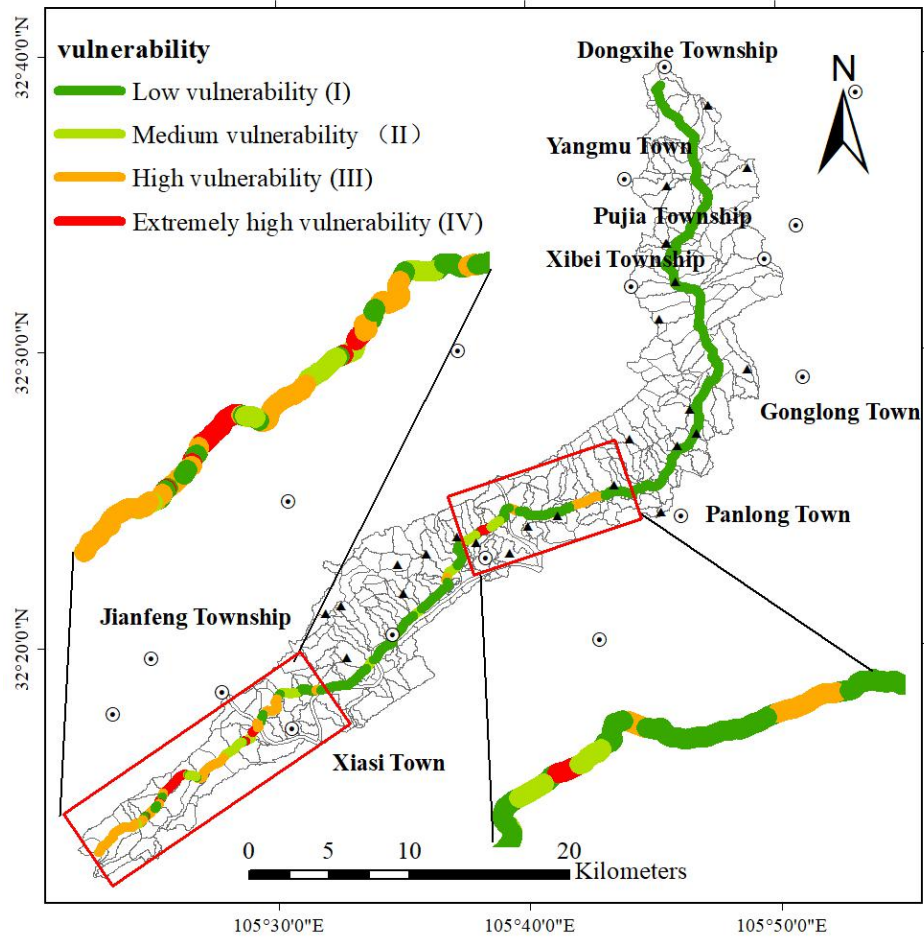
604

605

606

607

Figure 5

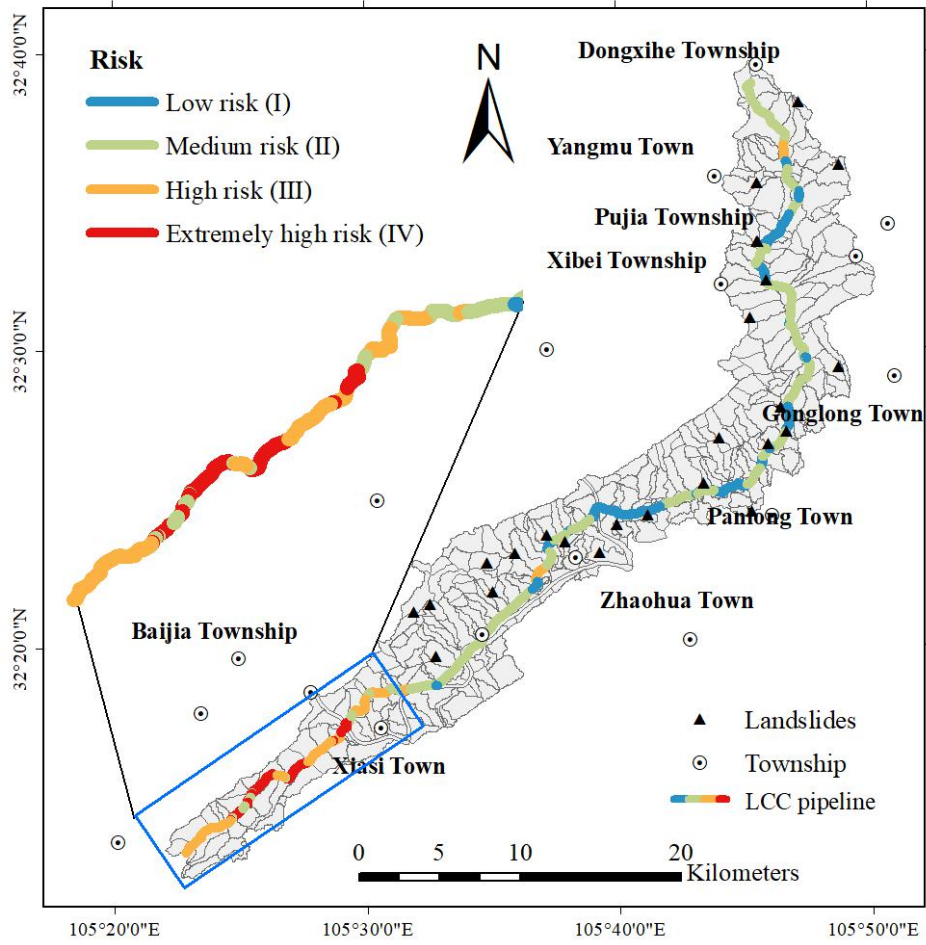


608

609

610

Figure 6



611
 612
 613
 614

Figure 7

Appendix 1 Classification of landslide susceptibility grade corresponding to different intervals

Factor	Indicators	Interval	Susceptibility degree monotonicity	Susceptibility level	
Landform	Elevation	[1000 , Highest]	Decreasing	Low susceptibility(I)	
		[Lowest , 600)	Increasing	Medium susceptibility(II)	
		[800 , 1000)	Decreasing	High susceptibility(III)	
		[600 , 700) \cup [700 , 800)	Increasing, Decreasing	Extremely high susceptibility(IV)	
	Slope	[60 , 90)	Decreasing	Low susceptibility(I)	
		[0 , 15)	Increasing	Medium susceptibility(II)	
		[30 , 60)	Decreasing	High susceptibility(III)	
		[15 , 20) \cup [20 , 30)	Increasing, Decreasing	Extremely high susceptibility(IV)	
		[0 , 45) \cup [270 , 360)	Increasing, Decreasing	Low susceptibility(I)	
		[225 , 270) \cup [45 , 90)	Decreasing, Increasing	Medium susceptibility(II)	
	Aspect	[90 , 135) \cup [180 , 225)	Increasing, Decreasing	High susceptibility(III)	
		[135 , 157.5) \cup [157.5 , 180)	Increasing, Decreasing	Extremely high susceptibility(IV)	
		[Lowest , 100)	Increasing	Low susceptibility(I)	
		[900 , Highest] \cup [100 , 200)	Decreasing, Increasing	Medium susceptibility(II)	
		[600 , 900) \cup [200 , 300)	Decreasing, Increasing	High susceptibility(III)	
		[300 , 450) \cup [450 , 600)	Increasing, Decreasing	Extremely high susceptibility(IV)	
		[Lowest , -0.025)	Increasing	Low susceptibility(I)	
		topographic profile curvature	[0.025 , Highest]	Decreasing	Medium susceptibility(II)
	[-0.025 , -0.01) \cup [0.01 , 0.025)		Increasing, Decreasing	High susceptibility(III)	
	[-0.01 , 0) \cup [0 , 0.01)		Increasing, Decreasing	Extremely high susceptibility(IV)	
	[-1,0)		Increasing	Low susceptibility(I)	
	Land cover	NDVI	[0,0.6) \cup [0.9,1]	Increasing, Decreasing	Medium susceptibility(II)
			[0.6,0.7) \cup [0.8,0.9)	Increasing, Decreasing	High susceptibility(III)
			[0.7,0.75) \cup [0.75,0.8)	Increasing, Decreasing	Extremely high susceptibility(IV)
[1100 , Highest)			Decreasing	Low susceptibility(I)	
Precipitation	Mean annual precipitation	[Lowest , 960)	Increasing	Medium susceptibility(II)	
		[990 , 1100)	Decreasing	High susceptibility(III)	
		[960 ,975) \cup [975 , 990)	Increasing,	Extremely high	

Geology	Distance from the fault	[20, Highest]	Decreasing	susceptibility(IV)
		[15 , 20)	Decreasing	Low susceptibility(I)
		[5 , 15)	Decreasing	Medium susceptibility(II)
		[0 ,5)	Decreasing	High susceptibility(III)
			Decreasing	Extremely high susceptibility(IV)

Appendix 2 Standard training sample matrix and standard test sample matrix

Sample type	ID	Input									Output
		Aspect	Slope	Elevation	NDVI	MAP	Height Difference	TPC	Distance	Lithology	
Training sample	1	0.2	89.9	438	-1	908.1	33	-0.582	25	1	0
	50	35.2	82.8	453	0	912.2	79	-0.456	23.47	1	0.06
	100	297.1	75.7	469	0.88	916.3	115	-0.33	21.9	1	0.12
	150	329.3	67.6	485	0.95	920.4	167	-0.168	20.34	1	0.19
	200	359.5	60	499	1	924.9	200	0.628	18.77	1	0.25
	250	68.4	3.8	1293	0.73	930.4	1097	0.486	17.21	2	0.31
	300	89.3	8.2	1206	0.65	938	1039	0.326	15.64	2	0.37
	350	246	12	1102	0.56	943.6	977	0.183	14.08	2	0.44
	400	269.3	15	1002	0.5	949.8	902	-0.142	12.52	2	0.5
	450	113.4	52.9	952	0.46	960.6	848	-0.018	10.95	3	0.56
500	134.8	46.3	905	0.4	972.6	757	-0.012	9.39	3	0.62	
Test sample	1	27.2	72.3	458	0.8	911.6	59	-0.544	25	1	0
	2	28.5	71.6	468	0.81	914.3	74	-0.453	23.69	1	0.06
	3	31.5	69.5	488	0.85	915.8	86	-0.381	22.37	1	0.11
	4	37.8	66.2	490	0.86	917.1	100	-0.228	21.06	1	0.16
	5	38.6	62.1	497	0.86	919.1	152	-0.03	19.74	1	0.22
	6	56.1	4.4	1141	0.7	934.2	939	0.439	18.43	2	0.27
	7	57.3	6.6	1240	0.68	939.6	941	0.429	17.11	2	0.32
	8	65.3	9.8	1257	0.66	945.1	1124	0.413	15.79	2	0.37
	9	68.2	11	1290	0.56	948.8	1135	0.318	14.48	2	0.43
	10	74.7	11.9	1382	0.53	949.9	1146	0.148	13.16	2	0.48
	11	92.4	30.4	848	0.47	963.4	613	-0.019	11.85	3	0.53
	12	92.7	31.8	853	0.45	970.5	683	-0.016	10.53	3	0.58
	13	101.9	44.7	900	0.45	980.5	737	-0.015	9.22	3	0.64

14	110.1	50.9	917	0.35	987	817	-0.015	7.9	3	0.69
15	115.6	57.5	933	0.32	994.2	835	-0.015	6.58	3	0.74
16	140.6	15.6	502	0.14	1001.5	245	0.019	5.27	4	0.79
17	155.4	20	626	0.14	1002.3	256	0.008	3.95	4	0.85
18	157.1	24.8	690	0.08	1010.6	293	0.007	2.64	4	0.9
19	177.6	27.3	765	0.06	1012.7	392	0.004	1.32	4	0.95
20	178.3	29.6	795	0.04	1022.7	446	0.001	0	4	1

618

619

Appendix 3 Test error of LM-BP neural network

Number	Expected value	network output	error
1	0	0.0006	0.0006
2	0.06	0.0548	-0.0052
3	0.11	0.1113	0.0013
4	0.16	0.1699	0.0099
5	0.22	0.2302	0.0102
6	0.27	0.2614	-0.0086
7	0.32	0.315	-0.005
8	0.37	0.3697	-0.0003
9	0.43	0.4266	-0.0034
10	0.48	0.4899	0.0099
11	0.53	0.5153	-0.0147
12	0.58	0.5765	-0.0035
13	0.64	0.6405	0.0005
14	0.69	0.701	0.011
15	0.74	0.7523	0.0123
16	0.79	0.8094	0.0194
17	0.85	0.8616	0.0116
18	0.9	0.9155	0.0155
19	0.95	0.9675	0.0175
20	1	1.0173	0.0173

622

Appendix 4 Coordinates of the center line and ancillary facilities of the pipeline

Point number	Previous point	Material	Diameter (mm)	Pressure	Depth (m)	Coordinate			elevation
						X	Y	H	
Marker peg		--	--	--	--	...576.265	...4357.849	503.877	--
GD1.421	GD1.420	Steel	168	high	2.2	...572.111	...4352.109	504.235	502.035
GD1.422	GD1.421	Steel	168	high	1.9	...571.837	...4336.010	503.866	501.966
GD1.423	GD1.422	Steel	168	high	2.1	...571.538	...4319.679	503.694	501.594
GD1.424	GD1.423	Steel	168	high	2.1	...571.093	...4308.825	503.510	501.410
GD1.425	GD1.424	Steel	168	high	2.0	...570.718	...4288.141	503.733	501.733
Detective pole K566		--	--	--	--	...575.536	...4284.069	503.494	--
GD1.426	GD1.425	Steel	168	high	2.3	...570.603	...4275.147	503.998	501.698
Mileage peg K566+200		--	--	--	--	...574.641	...4258.41	503.224	--
GD1.427	GD1.426	Steel	168	high	2.0	...570.222	...4258.593	503.710	501.710
GD1.428	GD1.427	Steel	168	high	1.6	...570.090	...4247.642	503.283	501.683
GD1.429	GD1.428	Steel	168	high	2.3	...569.458	...4216.618	502.468	500.168
GD1.430	GD1.429	Steel	168	high	2.9	...569.043	...4208.558	504.055	501.155

623

624

625

626

627

628

629

630

631

632

Appendix 5 Internal detection data of pipeline

FID	Pipe number	distance(m)	Feature type	Remarks	Length (mm)	thickness (mm)
1	10	6.408	Pipe segment	Spiral weld	652	11.1
2	20	7.060	Pipe segment	--	1178	--
3	20	7.648	Fixed punctuation point	Valve centerline	--	--
4	20	7.650	Valve	centerline	--	--
5	30	8.238	Pipe segment	Spiral weld	768	11.1
6	40	9.006	Pipe segment	--	2184	--
7	40	10.100	Globular tee	centerline	--	--
8	50	11.190	Pipe segment	Spiral weld	1700	11.1
9	50	11.445	Pit	--	548	11.1
10	60	12.890	Pipe segment	Straight weld	2342	13.6
11	60	12.890	Wall thickness variation	from 11.1mmto 13.6mm	--	--
13	70	15.232	Pipe segment	Spiral weld	1999	11.1
14	70	15.232	Wall thickness variation	from 13.6mmto 11.1mm	--	--
15	80	17.231	Pipe segment	Straight weld	2352	13.4
16	80	17.231	Wall thickness variation	from 11.1mmto 13.4mm	--	--
18	90	19.583	Pipe segment	Spiral weld	11557	11.1
19	90	19.583	Wall thickness variation	from 13.4mmto 11.1mm	--	--
20	90	28.060	Attachments	--	598	11.1
21	100	31.140	Pipe segment	--	991	--
22	100	31.580	Flange	centerline	--	--
23	110	32.131	Pipe segment	Spiral weld	11660	11.1
24	120	43.791	Pipe segment	Spiral weld	5536	11.1
25	130	49.327	Pipe segment	Straight weld	2213	16.2
26	130	49.327	Wall thickness variation	from 11.1mmto 16.2mm	--	--

28	140	51.540	Pipe segment	Spiral weld	5608	11.1
29	140	51.540	Wall thickness variation	from 16.2mmto 11.1mm	--	--
30	150	57.148	Pipe segment	Spiral weld	9432	11.1

634
635
636
637
638
639
640
641

Appendix 6 Core Code of Pipeline Defect Point Coordinate Calculating Program

```
642
643 using System;
644 using System.Collections.Generic;
645 using System.ComponentModel;
646 using System.Data;
647 using System.Drawing;
648 using System.Linq;
649 using System.Text;
650 using System.Threading.Tasks;
651 using System.Windows.Forms;
652 using System.IO;
653 private void button10_Click(object sender, EventArgs e)
654 {
655     double x1 = 0, y1 = 0, z1 = 0, x2 = 0, y2 = 0, z2 = 0, d1 = 0, d2 = 0, h1 = 0, h2 = 0;
656     double l = Convert.ToDouble(textBox9.Text);
657     double f = 0, nl=Convert.ToDouble(textBox7 .Text );
658     string[] SplitTxt = textBox2.Text.Split(',');
659     for (long i = 0; i < SplitTxt.Length-9; i+=5)
660     {
661         d1 = Convert.ToDouble(SplitTxt[i + 1]);
662         x1 = Convert.ToDouble(SplitTxt[i + 2]);
663         y1 = Convert.ToDouble(SplitTxt[i + 3]);
664         z1 = Convert.ToDouble(SplitTxt[i + 4]);
665         d2 = Convert.ToDouble(SplitTxt[i + 6]);
666         x2 = Convert.ToDouble(SplitTxt[i + 7]);
667         y2 = Convert.ToDouble(SplitTxt[i + 8]);
668         z2 = Convert.ToDouble(SplitTxt[i + 9]);
669         h1 = z1-d1;
670         h2 = z2-d2;
671         l += Math.Sqrt((x1-x2)*(x1-x2)+(y1-y2)*(y1-y2)+(h1-h2)*(h1-h2));
672     }
673     textBox8.Text =l.ToString();
674     f = (nl-l)/nl;
675     ff = f;
676     textBox5.Text = Convert.ToDouble(f ).ToString("P");
677 }
678 private void button9_Click(object sender, EventArgs e)
679 {
680     double fl = ff ;
681     double ll = 0;
682     string zb = ""; string[] SplitTxt = textBox3.Text.Split(',');
683     for (long i = 0; i < SplitTxt.Length - 1; i += 2)
684     {
685         ll = Convert.ToDouble(SplitTxt[i + 1]);
```

```

686         l1 += (-ff) * l1;
687         double x1 = 0, y1 = 0, z1 = 0, x2 = 0, y2 = 0, z2 = 0, d1 = 0, d2 = 0, h1 = 0, h2 = 0,
688         l0=0,l2=0;
689         double l = Convert.ToDouble(textBox9.Text);
690         double x = 0, y = 0, h = 0;
691         string[] SplitTxt1 = textBox2.Text.Split(',');
692         for (long j = 0; j < SplitTxt1.Length - 9; j += 5)
693         {
694             d1 = Convert.ToDouble(SplitTxt1[j + 1]);
695             x1 = Convert.ToDouble(SplitTxt1[j + 2]);
696             y1 = Convert.ToDouble(SplitTxt1[j + 3]);
697             z1 = Convert.ToDouble(SplitTxt1[j + 4]);
698             d2 = Convert.ToDouble(SplitTxt1[j + 6]);
699             x2 = Convert.ToDouble(SplitTxt1[j + 7]);
700             y2 = Convert.ToDouble(SplitTxt1[j + 8]);
701             z2 = Convert.ToDouble(SplitTxt1[j + 9]);
702             h1 = z1 - d1; h2 = z2 - d2;
703             l0= Math.Sqrt((x1 - x2) * (x1 - x2) + (y1 - y2) * (y1 - y2) + (h1 - h2) * (h1 - h2));
704             l = l + l0;
705             if (l - l1 < 0)
706             {
707                 ;
708             }
709             else if (l - l1 > 0)
710             {
711                 l2 = l0 - (l - l1);
712                 x = x1 + (x2 - x1) * l2 / l0;
713                 y = y1 + (y2 - y1) * l2 / l0;
714                 h = h1 + (h2 - h1) * l2 / l0;
715                 string xx, yy, hh, v;
716                 v = SplitTxt[i];
717                 xx = Convert.ToDouble(x).ToString();
718                 yy = Convert.ToDouble(y).ToString();
719                 hh = Convert.ToDouble(h).ToString();
720                 zb +=v + ","+ xx + ","+ yy + ","+ hh + "\n";
721                 break;
722             }
723         }
724     }
725     textBox6.Text = zb;
726 }

```

Appendix 7 Pipeline Landslide Risk Assessment Results

Fid	Start	Terminus	Susceptibility	Susceptibility level	Vulnerability	Vulnerability level	Risk	Risk level
1	K558	K559+446	0.874	IV	0.168	I	0.147	II
2	K559+446	K563+718	0.874	IV	0.178	I	0.156	II
3	K563+718	K564+883	0.932	IV	0.143	I	0.133	II
4	K564+883	K566+90	0.943	IV	0.149	I	0.141	II
5	K566+90	K567+117	0.943	IV	0.280	II	0.264	III
6	K567+117	K567+224	0.766	IV	0.095	I	0.073	I
7	K567+224	K567+384	0.729	III	0.117	I	0.085	II
8	K567+384	K567+674	0.729	III	0.079	I	0.058	I
9	K567+674	K567+782	0.729	III	0.141	I	0.103	II
10	K567+782	K567+846	0.729	III	0.066	I	0.048	I
11	K567+846	K567+904	0.729	III	0.097	I	0.071	I
12	K568+904	K568+197	0.722	III	0.154	I	0.111	II
13	K568+197	K568+430	0.763	IV	0.144	I	0.110	II
14	K569+430	K569+419	0.739	III	0.186	I	0.137	II
15	K569+419	K569+443	0.739	III	0.141	I	0.104	II
16	K569+443	K569+467	0.739	III	0.107	I	0.079	II
17	K569+467	K569+578	0.739	III	0.121	I	0.089	II
18	K569+578	K569+920	0.739	III	0.107	I	0.079	II
19	K571+920	K571+123	0.736	III	0.127	I	0.093	II
20	K571+123	K571+982	0.799	IV	0.109	I	0.087	II
21	K572+982	K572+729	0.753	IV	0.090	I	0.068	I
22	K573+729	K573+548	0.802	IV	0.094	I	0.075	I
23	K574+548	K574+249	0.805	IV	0.084	I	0.068	I
24	K574+249	K574+525	0.805	IV	0.150	I	0.121	II
25	K575+525	K575+538	0.805	IV	0.115	I	0.093	II
26	K575+538	K575+600	0.805	IV	0.157	I	0.126	II
27	K576+600	K576+737	0.816	IV	0.108	I	0.088	II
28	K577+737	K577+120	0.889	IV	0.089	I	0.079	I
29	K577+120	K577+146	0.889	IV	0.094	I	0.084	I
30	K577+146	K577+187	0.889	IV	0.169	I	0.150	II
31	K578+187	K578+571	0.889	IV	0.118	I	0.105	II
32	K578+571	K578+608	0.889	IV	0.095	I	0.084	I
33	K579+608	K579+624	0.853	IV	0.133	I	0.113	II
34	K580+624	K580+582	0.871	IV	0.156	I	0.136	II
35	K581+582	K581+43	0.871	IV	0.097	I	0.084	I
36	K581+43	K581+273	0.871	IV	0.143	I	0.125	II
37	K581+273	K581+536	0.880	IV	0.125	I	0.110	II
38	K581+536	K581+659	0.872	IV	0.154	I	0.134	II
39	K582+659	K582+263	0.830	IV	0.152	I	0.126	II
40	K582+263	K582+437	0.830	IV	0.116	I	0.096	II
41	K583+437	K583+512	0.830	IV	0.152	I	0.126	II
42	K583+512	K583+693	0.798	IV	0.105	I	0.084	II
43	K583+693	K583+720	0.740	III	0.113	I	0.084	II
44	K585+720	K585+55	0.740	III	0.178	I	0.132	II
45	K585+55	K585+101	0.668	III	0.196	I	0.131	II
46	K585+101	K585+370	0.668	III	0.178	I	0.119	II
47	K585+370	K585+634	0.696	III	0.190	I	0.132	II
48	K585+634	K585+734	0.668	III	0.116	I	0.077	II

49	K585+734	K585+908	0.627	III	0.198	I	0.124	II
50	K585+908	K585+949	0.627	III	0.168	I	0.105	II
51	K586+949	K586+782	0.627	III	0.173	I	0.108	II
52	K586+782	K586+805	0.627	III	0.117	I	0.073	II
53	K587+805	K587+364	0.627	III	0.171	I	0.107	II
54	K587+364	K587+498	0.618	III	0.078	I	0.048	I
55	K587+498	K587+794	0.618	III	0.107	I	0.066	I
56	K589+794	K589+251	0.618	III	0.102	I	0.063	I
57	K590+251	K590+757	0.618	III	0.172	I	0.106	II
58	K590+757	K590+780	0.556	III	0.153	I	0.085	II
59	K590+780	K590+812	0.556	III	0.123	I	0.068	II
60	K591+812	K591+500	0.555	III	0.135	I	0.075	II
61	K591+500	K591+946	0.555	III	0.087	I	0.048	I
62	K592+946	K592+259	0.555	III	0.107	I	0.059	I
63	K593+259	K593+631	0.517	III	0.152	I	0.079	II
64	K593+631	K593+912	0.374	II	0.153	I	0.057	II
65	K594+912	K594+993	0.374	II	0.150	I	0.056	II
66	K595+993	K595+203	0.374	II	0.076	I	0.028	I
67	K595+203	K595+261	0.359	II	0.114	I	0.041	I
68	K595+261	K595+383	0.359	II	0.099	I	0.036	I
69	K596+383	K596+383	0.412	II	0.278	II	0.115	II
70	K596+383	K596+429	0.412	II	0.107	I	0.044	I
71	K597+429	K597+62	0.359	II	0.121	I	0.043	I
72	K597+62	K597+200	0.412	II	0.158	I	0.065	II
73	K597+200	K597+345	0.412	II	0.133	I	0.055	I
74	K597+345	K597+680	0.412	II	0.273	II	0.112	II
75	K599+680	K599+376	0.321	II	0.461	II	0.148	II
76	K599+376	K599+693	0.211	I	0.105	I	0.022	I
77	K600+693	K600+188	0.211	I	0.179	I	0.038	I
78	K600+188	K600+353	0.106	I	0.172	I	0.018	I
79	K601+353	K601+369	0.106	I	0.264	II	0.028	I
80	K602+369	K602+495	0.099	I	0.190	I	0.019	I
81	K603+495	K603+131	0.067	I	0.436	II	0.029	I
82	K603+131	K603+551	0.099	I	0.144	I	0.014	I
83	K604+551	K604+321	0.104	I	0.253	II	0.026	I
84	K604+321	K604+976	0.099	I	0.102	I	0.010	I
85	K605+976	K605+735	0.178	I	0.372	II	0.066	II
86	K606+735	K606+368	0.236	I	0.637	III	0.150	II
87	K606+368	K606+838	0.236	I	0.127	I	0.030	I
88	K607+838	K607+596	0.323	II	0.407	II	0.131	II
89	K608+596	K608+20	0.323	II	0.163	I	0.053	II
90	K608+20	K608+287	0.323	II	0.145	I	0.047	I
91	K608+287	K608+546	0.346	II	0.084	I	0.029	I
92	K608+546	K608+583	0.406	II	0.215	I	0.087	II
93	K608+583	K608+835	0.406	II	0.291	II	0.118	II
94	K609+835	K609+565	0.442	II	0.279	II	0.123	II
95	K610+565	K610+564	0.442	II	0.403	II	0.178	II
96	K610+564	K610+945	0.442	II	0.453	II	0.200	II
97	K611+945	K611+89	0.482	II	0.117	I	0.056	I
98	K611+89	K611+691	0.501	III	0.138	I	0.069	II
99	K612+691	K612+413	0.501	III	0.175	I	0.088	II

100	K613+413	K613+269	0.501	III	0.163	I	0.082	II
101	K613+269	K613+442	0.502	III	0.166	I	0.083	II
102	K614+442	K614+83	0.502	III	0.354	II	0.178	II
103	K614+83	K614+980	0.502	III	0.263	II	0.132	II
104	K615+980	K615+218	0.601	III	0.153	I	0.092	II
105	K615+218	K615+388	0.601	III	0.143	I	0.086	II
106	K616+388	K616+87	0.635	III	0.126	I	0.080	II
107	K616+87	K616+300	0.556	III	0.144	I	0.080	II
108	K616+300	K616+460	0.505	III	0.269	II	0.136	II
109	K617+460	K617+715	0.505	III	0.172	I	0.087	II
110	K617+715	K617+827	0.505	III	0.255	II	0.129	II
111	K618+827	K618+28	0.556	III	0.170	I	0.095	II
112	K618+28	K618+687	0.556	III	0.313	II	0.174	II
113	K620+687	K620+78	0.556	III	0.188	I	0.105	II
114	K620+78	K620+298	0.425	II	0.196	I	0.083	II
115	K621+298	K621+509	0.576	III	0.223	I	0.128	II
116	K621+509	K621+611	0.425	II	0.107	I	0.045	I
117	K622+611	K622+10	0.425	II	0.262	II	0.111	II
118	K622+10	K622+86	0.425	II	0.122	I	0.052	I
119	K622+86	K622+539	0.693	III	0.178	I	0.123	II
120	K622+539	K622+897	0.634	III	0.549	III	0.348	III
121	K623+897	K623+36	0.634	III	0.535	III	0.339	III
122	K623+36	K623+794	0.693	III	0.145	I	0.100	II
123	K624+794	K624+866	0.693	III	0.310	II	0.215	II
124	K625+866	K625+242	0.796	IV	0.137	I	0.109	II
125	K627+242	K627+60	0.859	IV	0.452	II	0.388	III
126	K627+60	K627+162	0.859	IV	0.193	I	0.166	II
127	K627+162	K627+313	0.859	IV	0.166	I	0.143	II
128	K627+313	K627+700	0.783	IV	0.167	I	0.131	II
129	K628+700	K628+146	0.908	IV	0.501	III	0.455	III
130	K628+146	K628+196	0.908	IV	0.139	I	0.126	II
131	K628+196	K628+610	0.908	IV	0.631	III	0.573	IV
132	K629+610	K629+355	0.787	IV	0.369	II	0.290	III
133	K629+355	K629+525	0.787	IV	0.729	III	0.574	IV
134	K629+525	K629+570	0.787	IV	0.252	II	0.198	II
135	K629+570	K629+620	0.787	IV	0.465	II	0.366	III
136	K630+620	K630+348	0.787	IV	0.286	II	0.225	II
137	K630+348	K630+956	0.892	IV	0.389	II	0.347	III
138	K631+956	K631+116	0.886	IV	0.423	II	0.375	III
139	K631+116	K631+528	0.805	IV	0.513	III	0.413	III
140	K633+528	K633+435	0.805	IV	0.568	III	0.457	III
141	K635+435	K635+302	0.933	IV	0.625	III	0.583	IV
142	K635+302	K635+326	0.884	IV	0.611	III	0.540	III
143	K635+326	K635+359	0.884	IV	0.441	II	0.390	III
144	K635+359	K635+368	0.884	IV	0.194	I	0.171	II
145	K635+368	K635+530	0.884	IV	0.374	II	0.331	III
146	K635+530	K635+604	0.884	IV	0.307	II	0.271	III
147	K635+604	K635+850	0.805	IV	0.377	II	0.303	III
148	K635+850	K635+943	0.805	IV	0.234	I	0.188	II
149	K635+943	K635+972	0.805	IV	0.139	I	0.112	II
150	K635+972	K635+974	0.805	IV	0.121	I	0.097	II

151	K635+974	K635+990	0.805	IV	0.138	I	0.111	II
152	K636+990	K636+152	0.933	IV	0.598	III	0.558	III
153	K636+152	K636+159	0.933	IV	0.157	I	0.146	II
154	K636+159	K636+320	0.884	IV	0.579	III	0.512	III
155	K636+320	K636+427	0.884	IV	0.166	I	0.147	II
156	K636+427	K636+517	0.884	IV	0.124	I	0.110	II
157	K636+517	K636+806	0.834	IV	0.663	III	0.553	III
158	K636+806	K636+893	0.834	IV	0.794	IV	0.662	IV
159	K637+893	K637+57	0.834	IV	0.519	III	0.433	III
160	K637+57	K637+109	0.834	IV	0.542	III	0.452	III
161	K637+109	K637+181	0.834	IV	0.111	I	0.093	II
162	K637+181	K637+332	0.834	IV	0.127	I	0.106	II
163	K638+332	K638+87	0.834	IV	0.608	III	0.507	III
164	K638+87	K638+140	0.834	IV	0.157	I	0.131	II
165	K638+140	K638+193	0.767	IV	0.682	III	0.523	III
166	K638+193	K638+199	0.767	IV	0.188	I	0.144	II
167	K638+199	K638+226	0.767	IV	0.126	I	0.097	II
168	K638+226	K638+368	0.767	IV	0.532	III	0.408	III
169	K638+368	K638+409	0.767	IV	0.604	III	0.463	III
170	K638+409	K638+432	0.767	IV	0.205	I	0.157	II
171	K638+432	K638+444	0.767	IV	0.525	III	0.403	III
172	K638+444	K638+676	0.767	IV	0.173	I	0.133	II
173	K638+676	K638+837	0.767	IV	0.479	II	0.367	III
174	K639+837	K639+266	0.744	III	0.483	II	0.359	III
175	K639+266	K639+339	0.744	III	0.427	II	0.318	III
176	K639+339	K639+435	0.744	III	0.549	III	0.408	III
177	K639+435	K639+562	0.631	III	0.324	II	0.204	II
178	K640+562	K640+63	0.607	III	0.476	II	0.289	III
179	K641+63	K641+600	0.607	III	0.604	III	0.367	III
180	K642+600	K642+225	0.607	III	0.461	II	0.280	III

728

729

730

Appendix 8 Field environment of study area



731

732

Figure 1 Vegetation distribution in a watershed of the study area



733

734

Figure 2 Vegetation environment of a pipeline section in the study area



735

736

Figure 3 Outcropping of rock strata in the study area